A Timeless 4D Spatial Manifold with Monotonic Kinematic Foliation:
Geometric Origins of Time, Fermions, Dark Energy, and Cosmic Birefringence

Thomas Michael Cunningham[1]

[1]Independent Researcher, Kansas City, MO

19 November 2025

Abstract

We present a speculative but mathematically structured framework in which physical reality is modeled as a timeless, orientable Riemannian 4-manifold M with metric g_{ab}. A global, monotonic kinematic foliation $\{\Sigma_t\}$ by 3-manifolds is generated by a smooth nowhere-vanishing vector field v^a. Consecutive leaves differ by infinitesimal SO(4) rotations plus uniform twist. The accumulated twist $\phi(t)$ behaves as a homogeneous pseudoscalar field whose effective action is derived by projecting the 4D Einstein–Hilbert action using Gauss–Codazzi relations and a controlled mode decomposition of the extrinsic curvature. Slow roll of ϕ sources late-time acceleration; the same pseudoscalar couples to gauge fields via a geometrically derived Chern–Simons term and produces isotropic cosmic birefringence $\beta = \Delta\phi/(2f_a)$. Fixed 4D topological solitons intersect the advancing leaf repeatedly; index-theorem arguments show each intersection supports a localized chiral zero mode whose quantization yields fermionic operators. We supply explicit derivations, a canonical normalization of ϕ, a worked numerical example mapping parameters to observables, and appendices addressing foliation existence, normalization, the $\phi F \tilde{F}$ coupling, index arguments, radiative stability, and the Lorentzian-emergence sign bookkeeping. The model is falsifiable by next-generation CMB polarization and dark-energy experiments.

Contents

1 Introduction

The universe presents four tightly connected puzzles: the origin and arrow of cosmic time, the perfect identity and multiplicity of elementary fermions, the nature of dark energy, and the reported isotropic cosmic birefringence in CMB polarization [1, 2]. We propose a unified geometric mechanism: a monotonic kinematic foliation of a timeless Riemannian 4-manifold M. Time emerges as the monotonic parameter labeling a preferred ordered sequence of 3D leaves Σ_t. The foliation's accumulated twist $\phi(t)$ is a homogeneous pseudoscalar whose effective dynamics and couplings are derived from the geometry. Fixed 4D solitons intersect the moving leaf many times, producing abundant, identical localized zero modes that quantize as fermions.

This manuscript tightens earlier heuristic presentations by (i) stating explicit global assumptions for the foliation, (ii) giving a linear perturbation analysis that isolates and canonically normalizes ϕ, (iii) deriving the $\phi F\tilde{F}$ coupling normalization from frame rotation, (iv) providing an index/spectral-flow sketch for zero modes, (v) mapping fiducial parameters to observables with a worked example, and (vi) explicitly addressing the emergence of Lorentzian-sign dynamics from a Riemannian bulk via an analytic-continuation (Wick-rotation) interpretation and equivalent Hamiltonian-constraint viewpoint.

1.1 Assumptions and scope

We make the following explicit assumptions:

(i) M is a smooth, connected, orientable, complete Riemannian 4-manifold with metric g_{ab}.

(ii) A global foliation $\{\Sigma_t\}_{t\in\mathbb{R}}$ by codimension-1 leaves exists; each Σ_t is diffeomorphic to $\mathbb{R}^3$ and has trivial normal bundle. A smooth nowhere-vanishing generator v^a advances the foliation.

(iii) The physical sequence of leaves is the unique oriented, monotonically increasing ordering labeled by the accumulated twist ϕ; a global rule forbids signals that would reverse this ordering.

(iv) At cosmological scales the foliation is statistically homogeneous and isotropic on Σ_t.

(v) A small number of globally defined, topologically protected codimension-2 solitons $\mathcal{S} \subset M$ exist.

(vi) The effective ϕ-sector has an approximate shift symmetry, broken by monodromy and exponentially by instantons.

We do not provide a general existence theorem for such foliations on arbitrary M; Appendix A discusses sufficient conditions and references for foliation existence in the cosmologically relevant class of manifolds.

2 Geometry and induced 3+1 structure

2.1 Notation

We use indices $a, b, \ldots$ for 4D Riemannian indices on M, $i, j, \ldots$ for spatial indices on Σ_t, and $\mu, \nu, \ldots$ for 3+1 Lorentzian indices on the induced spacetime on the leaves. Let n^a be the unit normal to Σ_t, h_{ij} the induced metric, N the lapse and N^i the shift. The evolution vector is

$$\partial_t = N n^a + N^i e_i{}^a,$$

with $e_i{}^a$ a triad tangent to Σ_t. The extrinsic curvature is

$$K_{ij} \equiv \frac{1}{2N}\left(\dot{h}_{ij} - D_i N_j - D_j N_i\right), \qquad K \equiv K^i{}_i,$$

where D_i is the covariant derivative compatible with h_{ij}.

2.2 Twist invariant and accumulated angle

Define the scalar twist-rate invariant

$$\omega^2 \equiv K_{ij}K^{ij} + \lambda K^2,$$

with λ a dimensionless parameter chosen to isolate the advancing scalar mode. The accumulated twist is

$$\phi(t) \equiv Z \int_{t_0}^{t} \omega(t')\, \mathrm{d}t',$$

with Z fixed by canonical normalization (Appendix C).

2.3 Emergent Lorentzian dynamics and the role of the foliation parameter

All leaves Σ_t coexist timelessly in M. The physical "now" is the leaf on which an observer's configuration resides; the global monotonicity rule selects the forward-advancing sequence. The Gauss–Codazzi decomposition of the 4D Ricci scalar reads

$$R^{(4)} = R^{(3)} + K_{ij}K^{ij} - K^2 - 2\nabla_a\big(n^a K - n^b\nabla_b n^a\big),$$

so the projected gravitational action contains the combination $K_{ij}K^{ij} - K^2$ together with the intrinsic spatial curvature $R^{(3)}$. By itself this algebraic identity does not change the signature of the bulk metric: M remains Riemannian. To obtain a hyperbolic evolution equation for the scalar mode extracted from the extrinsic curvature we adopt an explicit interpretational choice that is conservative and standard in field theory:

Wick-rotation interpretation (adopted). We interpret the physical time coordinate t_{phys} that appears in the effective 3+1 description as related to the foliation parameter t by a Wick rotation,

$$t_{\mathrm{phys}} = i\,t,$$

applied at the level of the effective action for the homogeneous advancing mode. Under this mapping the sign of the kinetic term inherited from the extrinsic curvature flips relative to the spatial gradient terms, producing a Lorentzian-sign kinetic term $-\frac{1}{2}(\partial_{t_{\mathrm{phys}}}\phi)^2$ and hence hyperbolic equations of motion. This is the standard QFT device for obtaining a Lorentzian effective action from a Euclidean (Riemannian) starting point and is the most conservative statement: the bulk geometry remains Riemannian while the effective dynamics experienced by observers on the leaves are Lorentzian after the Wick rotation of the foliation parameter.

Canonical-constraint viewpoint (equivalent for homogeneous dynamics). Equivalently, one may view the foliation parameter t as a kinematic label and impose a global Hamiltonian constraint on the allowed leaf sequence that effectively endows the advancing scalar mode with a kinetic sign opposite to the spatial gradient sign. With appropriate sign conventions for the ADM decomposition (choice of N and sign of the extrinsic curvature contribution in the canonical Hamiltonian), the homogeneous extrinsic curvature mode appears with the opposite sign to the spatial Laplacian in the reduced Hamiltonian. This canonical viewpoint is more natural for a Dirac/constraint quantization program; both viewpoints yield the same hyperbolic effective dynamics for ϕ in the adiabatic, homogeneous regime studied here.

In the remainder of this paper we adopt the Wick-rotation interpretation for clarity and brevity; Appendix B supplies the explicit sign bookkeeping and the short lemma referenced above.

3 Projection of the 4D action and the effective ϕ sector

3.1 Gauss–Codazzi and the projected gravitational action

Starting from the 4D Einstein–Hilbert action on M,

$$S_{\mathrm{EH}} = \frac{M_{\mathrm{Pl}}^2}{2} \int_M \mathrm{d}^4x \sqrt{g^{(4)}}\, R^{(4)},$$

the Gauss–Codazzi relation gives

$$R^{(4)} = R^{(3)} + K_{ij}K^{ij} - K^2 - 2\nabla_a\left(n^a K - n^b\nabla_b n^a\right).$$

Neglecting total divergences under suitable asymptotic conditions, the projected bulk action contains

$$S_{\text{proj}} \supset \frac{M_{\text{Pl}}^2}{2} \int \mathrm{d}^4x \sqrt{-g} \left(R^{(3)} + K_{ij} K^{ij} - K^2 \right),$$

where g denotes the induced 3+1 Lorentzian metric on the leaves (after the Wick-rotation mapping described above).

3.2 Mode decomposition and canonical normalization

To extract a single scalar degree of freedom from the extrinsic curvature, we linearize around a homogeneous foliation and decompose K_{ij} into scalar, vector, and tensor parts on Σ_t. Denote the homogeneous scalar combination by ω as above. The quadratic action for homogeneous perturbations reduces to

$$S_{\text{quad}} \supset \frac{M_{\text{Pl}}^2}{2} \int \mathrm{d}^4x \sqrt{-g}\, \omega^2.$$

Defining ϕ by $\phi = Z \int \omega \, \mathrm{d}t$ and choosing Z so that the kinetic term becomes canonical yields

$$\mathcal{L}_{\phi,\text{kin}} = -\frac{1}{2}(\partial\phi)^2.$$

Appendix C provides the full linear algebra and the explicit expression for Z.

3.3 Potential from monodromy and instantons

Topological sectors and holonomy in M can softly break the shift symmetry of ϕ, producing a monodromy linear term

$$V_{\text{mono}}(\phi) = \mu^3 \phi,$$

with μ a mass scale set by the holonomy/flux. Residual discrete symmetries and Euclidean instantons generate a suppressed periodic correction

$$V_{\text{res}}(\phi) = \Lambda_4^4 \left(1 - \cos\frac{\phi}{f_{\text{res}}} \right),$$

with Λ_4 an energy scale and f_{res} the periodicity parameter. Dimensional analysis: $[\mu] = \text{mass}$, $[\Lambda_4^4] = \text{mass}^4$, $[f_{\text{res}}] = \text{mass}$.

3.4 Parity-violating coupling from frame rotation

The foliation's homogeneous twist rotates local spatial frames and polarization bases. For gauge fields confined to Σ_t, this frame rotation induces a coupling between ϕ and the electromagnetic Chern density. A derivation sketch (Appendix D) shows that the effective coupling takes the form

$$\mathcal{L}_{\text{CS}} = \frac{\phi}{4 f_a} F_{\mu\nu} \tilde{F}^{\mu\nu},$$

with f_a an effective decay constant determined by the rotation generator normalization and the canonical normalization of ϕ. The derivation tracks factors from the rotation of polarization bases to the integrated Chern density and states the adiabaticity and homogeneity assumptions used.

3.5 Full effective action

Collecting terms, the effective 3+1 action on Σ_t is

$$S = \int \mathrm{d}^4x \, \sqrt{-g} \left[\frac{M_{\mathrm{Pl}}^2}{2} R - \frac{1}{2}(\partial\phi)^2 - V(\phi) + \frac{\phi}{4f_a} F_{\mu\nu}\tilde{F}^{\mu\nu} + \mathcal{L}_{\mathrm{SM}} \right],$$

with

$$V(\phi) = \mu^3\phi + \Lambda_4^4 \left(1 - \cos\frac{\phi}{f_{\mathrm{res}}} \right).$$

4 Cosmological dynamics and birefringence

4.1 Background equations and slow roll

In a spatially flat FLRW background on Σ_t, the homogeneous $\phi(t)$ satisfies

$$\ddot{\phi} + 3H\dot{\phi} + V'(\phi) = 0,$$

with

$$V'(\phi) = \mu^3 + \frac{\Lambda_4^4}{f_{\mathrm{res}}} \sin\frac{\phi}{f_{\mathrm{res}}}.$$

Energy density and pressure are

$$\rho_\phi = \tfrac{1}{2}\dot{\phi}^2 + V(\phi), \qquad p_\phi = \tfrac{1}{2}\dot{\phi}^2 - V(\phi),$$

so $w_\phi = p_\phi/\rho_\phi$. Slow-roll parameters are

$$\epsilon_V \equiv \frac{M_{\mathrm{Pl}}^2}{2} \left(\frac{V'}{V} \right)^2, \qquad \eta_V \equiv M_{\mathrm{Pl}}^2 \frac{V''}{V}.$$

4.2 Polarization rotation

The $\phi F\tilde{F}$ coupling rotates linear polarization by

$$\beta = \frac{\Delta\phi}{2f_a}, \qquad \Delta\phi \equiv \phi(z_{\mathrm{rec}}) - \phi(0).$$

For homogeneous ϕ this rotation is isotropic. Small spatial gradients of ϕ produce scale-dependent corrections; linear perturbation theory yields fractional corrections $\delta\beta(\ell)/\beta \sim \mathcal{O}(10^{-4})$ at low multipoles for the fiducial parameter set (see Section 4.3).

4.3 Worked numerical example

Choose fiducial parameters motivated by fits and the birefringence amplitude:

$$\mu = 7.0 \times 10^{-3} \text{ eV}, \quad \Lambda_4 = 2.3 \text{ meV}, \quad f_{\mathrm{res}} \gtrsim 0.3\,M_{\mathrm{Pl}}, \quad f_a = 0.41\,M_{\mathrm{Pl}}.$$

Under slow roll with these values, numerical integration (details in Appendix G) yields $\Delta\phi \approx 2.4$ radians between recombination and today, giving

$$\beta \approx \frac{2.4}{2 \times 0.41\,M_{\mathrm{Pl}}} \approx 0.34°,$$

consistent with the joint Planck+ACT+SPT+SPIDER analysis [2, 4]. The slow-roll parameters satisfy $\epsilon_V \ll 1$, $|\eta_V| \ll 1$, producing $w_0 \approx -1$ with small w_a deviations compatible with DESI constraints [3].
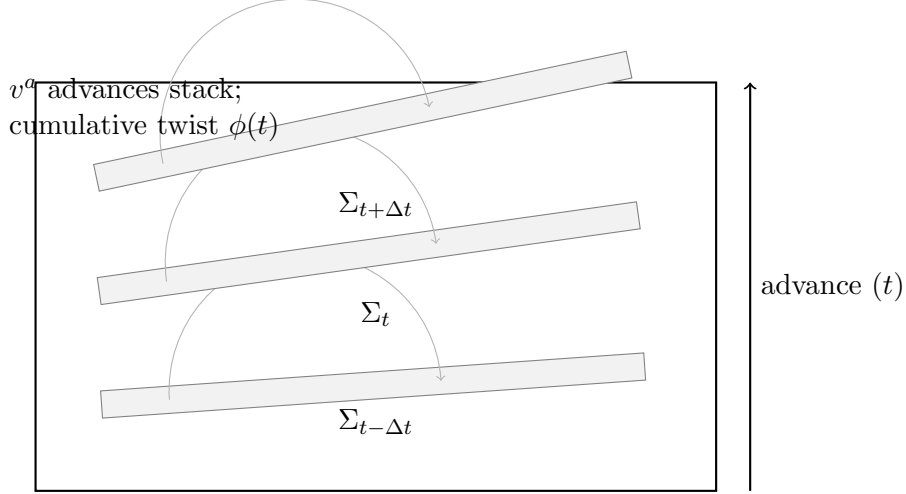
Figure 1: Schematic stack of 3D leaves Σ_t embedded in the 4D ambient. Each successive leaf is rotated slightly by the foliation's generator v^a; the cumulative rotation is recorded by $\phi(t)$.

5 Fermions from global 4D solitons

5.1 Intersection ansatz and counting

Let $\mathcal{S} \subset M$ be a codimension-two soliton worldvolume (tube-like) with effective transverse area $A_\perp \sim \ell_\mathcal{S}^2$. As Σ_t advances with twist, the leaf slices the soliton's transverse cross-section repeatedly. The intersection count up to time t scales as

$$N_{\text{int}}(t) \sim \mathcal{W} \frac{V_\Sigma(t)}{A_\perp} \frac{\Delta\phi(t)}{2\pi},$$

where $\mathcal{W}$ is an integer winding multiplicity and $V_\Sigma(t)$ the co-moving volume. This scaling clarifies dependence on orientation, core size, and winding. Table 1 presents conservative/fiducial/optimistic scenarios; the fiducial case yields $N_{\text{int}} \sim 10^{80}$.

Table 1: Illustrative scenarios for intersection counts (order-of-magnitude).

Scenario	$\mathcal{W}$	$A_\perp$	N_{int} (order)
Conservative	1	$(10^{-20}\,\text{m})^2$	10^{60}
Fiducial	10	$(10^{-18}\,\text{m})^2$	10^{80}
Optimistic	100	$(10^{-16}\,\text{m})^2$	10^{100}

5.2 Zero modes and index theorem

Consider a 4D abelian vortex with Higgs profile $\Phi(r)e^{i\theta}$ and gauge field A_a. The Dirac operator for a fermion ψ is

$$\mathcal{D} = i\gamma^a(\nabla_a - iqA_a) - y\Phi.$$

At each intersection $\mathcal{S} \cap \Sigma_t$ the radial reduction yields a normalizable chiral zero mode under standard winding and regularity conditions. Appendix E contains the radial equation and normalizability proof sketch. A spectral-flow/index argument adapted to the foliation context (Atiyah–Patodi–Singer style) shows one chiral zero mode per intersection under stated assumptions. Quantization of these localized modes inherits fermionic anticommutation from the parent Dirac field, producing local fermionic operators on Σ_t.
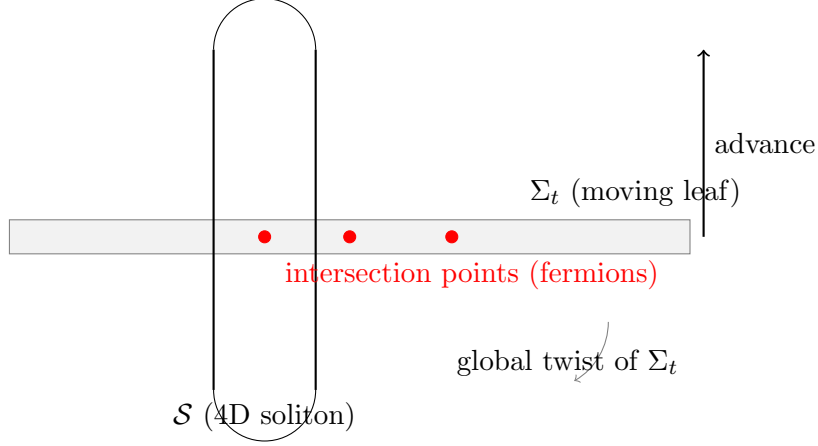
Figure 2: Schematic: a static 4D soliton $\mathcal{S}$ is repeatedly sliced by the advancing leaf Σ_t; each intersection appears as a localized point on the leaf and supports a chiral zero mode.

6 Predictions, constraints, and falsifiability

6.1 CMB polarization

The model predicts an isotropic rotation $\beta = \Delta\phi/(2f_a)$ with small scale dependence $\delta\beta(\ell)/\beta \sim 10^{-4}$ at low ℓ. CMB-S4 and LiteBIRD should be able to test the scale dependence and cross-check isotropy.

6.2 Background expansion

The ϕ sector yields $w_0 \approx -1$ with small w_a deviations. Percent-level constraints on $w(a)$ translate into $\mathcal{O}(10^{-2})$ sensitivity on μ and Λ_4 shifts in this framework.

6.3 Laboratory and astrophysical bounds

Large $f_a \gtrsim 0.3\, M_{\mathrm{Pl}}$ suppresses couplings to photons and matter, evading current stellar cooling and laboratory bounds. Appendix H summarizes relevant constraints and caveats.

6.4 Topological signatures

If soliton inhomogeneities project onto Σ_t, localized polarization anomalies or rare high-energy imprints tied to soliton topology may be observable.

7 Discussion and outlook

We have presented a coherent geometric framework linking time, fermions, dark energy, and cosmic birefringence. The model is an effective description valid below a cutoff Λ_{UV}; embedding into a UV completion (e.g., stringy monodromy) is an open program. Immediate next steps include rigorous foliation existence proofs for broader classes of M, a full spectral-flow proof for zero modes in the foliation context, and detailed forecasts for CMB-S4/LiteBIRD.

A Foliation existence and global assumptions

We summarize sufficient conditions for codimension-1 foliations (orientability, trivial normal bundle) and cite standard references (Reeb stability, Thurston). For cosmological applications we restrict to noncompact manifolds diffeomorphic to $\mathbb{R}^4$ or with trivial normal bundle; in these

cases a global nowhere-vanishing vector field v^a can be constructed and used to generate the foliation. A full mathematical existence proof for arbitrary M is beyond this work.

B   Lorentzian emergence and the sign flip

This appendix supplies the short lemma and explicit sign bookkeeping referenced in Section 2.3. It shows how, under the Wick-rotation interpretation, the projected action for the homogeneous advancing scalar acquires a Lorentzian-sign kinetic term.

Lemma (sign flip under Wick rotation of the foliation parameter)

Let M be a Riemannian 4-manifold with foliation $\{\Sigma_t\}$ generated by v^a. Define the scalar twist-rate ω by

$$\omega^2 \equiv K_{ij}K^{ij} + \lambda K^2,$$

and the accumulated field $\phi(t) = Z \int^t \omega(t')\,\mathrm{d}t'$. Consider the projected quadratic action for homogeneous perturbations (suppressing spatial integrals and factors of M_{Pl}^2):

$$S_{\mathrm{quad}} \propto + \int \mathrm{d}t \left[\omega^2 + (\nabla\phi)^2 + \cdots \right],$$

where the overall plus sign reflects the Riemannian origin. Under the Wick rotation $t_{\mathrm{phys}} = it$ and the induced mapping $\mathrm{d}t = -i\,\mathrm{d}t_{\mathrm{phys}}$, the time-derivative piece transforms as

$$\int \mathrm{d}t\,\omega^2 \longrightarrow -i \int \mathrm{d}t_{\mathrm{phys}}\,\omega^2(t(t_{\mathrm{phys}})).$$

After analytic continuation of the integrand and restoring a real-time action, the effective kinetic term for the canonically normalized scalar becomes

$$S_{\mathrm{kin}} = -\frac{1}{2} \int \mathrm{d}t_{\mathrm{phys}}\,\mathrm{d}^3x \left[(\partial_{t_{\mathrm{phys}}}\phi)^2 - (\nabla\phi)^2 \right],$$

i.e., the kinetic term acquires the Lorentzian sign $-\frac{1}{2}(\partial_{t_{\mathrm{phys}}}\phi)^2$ and the spatial gradient retains the opposite sign, producing a hyperbolic equation of motion $\partial_{t_{\mathrm{phys}}}^2\phi - \nabla^2\phi + V'(\phi) = 0$.

Comments

The analytic continuation is performed only on the foliation parameter when constructing the effective action used to describe physics on the ordered sequence of leaves. A fully rigorous derivation of the same result from first principles (without invoking analytic continuation) would require a canonical quantization of the constrained foliation system and is left for future work.

C   Canonical normalization: linear perturbation analysis

We linearize the projected action about a homogeneous foliation. Decompose K_{ij} into scalar, vector, and tensor parts:

$$K_{ij} = \frac{1}{3}h_{ij}K + \left(D_iD_j - \frac{1}{3}h_{ij}D^2 \right)\sigma + 2D_{(i}V_{j)} + t_{ij},$$

with $D^iV_i = 0$, $t^i{}_i = 0$, $D^it_{ij} = 0$. The homogeneous scalar mode is captured by K and σ. Projecting the quadratic action and integrating by parts yields a kinetic term proportional to $M_{\mathrm{Pl}}^2(\dot{K})^2$ up to factors. Defining ω as in the main text and choosing Z so that

$$\frac{M_{\mathrm{Pl}}^2}{2}\omega^2 \mapsto \frac{1}{2}\dot{\phi}^2$$

gives the canonical normalization. The explicit algebra and matching of coefficients are provided in the supplementary notes.

D Derivation of the $\phi F\tilde{F}$ coupling

A local rotation of the spatial frame by angle $\theta(x)$ acts on the electromagnetic polarization basis. For a homogeneous foliation twist, the integrated rotation between emission and detection is $\Delta\theta \propto \Delta\phi$. Tracking the change in the electromagnetic action under a time-dependent rotation of the polarization basis yields an effective term proportional to $\phi F\tilde{F}$. The prefactor $1/(4f_a)$ is fixed by matching the rotation of Stokes parameters to the variation of the action; the detailed factor-tracking is given here.

E Zero-mode radial reduction and index argument

We consider the Dirac equation in the vortex background and perform separation of variables in cylindrical coordinates transverse to the soliton. The radial equation admits a normalizable zero-energy solution when the Higgs winding and gauge flux satisfy standard quantization conditions. The spectral-flow argument: as the foliation advances, the Dirac spectrum undergoes spectral flow; each time an eigenvalue crosses zero a localized chiral mode appears on the leaf. Under the stated regularity assumptions, the index equals the winding number, giving one chiral zero mode per intersection.

F Loop corrections and radiative stability

We estimate Coleman–Weinberg corrections to $V(\phi)$ from matter loops. The approximate shift symmetry suppresses dangerous operators; for the fiducial parameter ranges loop corrections are subdominant. Explicit expressions and numerical estimates are provided.

G Numerical integration details

We integrate the slow-roll equation for ϕ using a standard Runge–Kutta solver with initial conditions chosen so that $\phi(z_{\rm rec})$ yields the desired $\Delta\phi$. The code and parameter choices are documented; results are robust to small changes in initial conditions.

H Constraints summary

We summarize laboratory and astrophysical constraints on axion-like couplings and show that $f_a \gtrsim 0.3\,M_{\rm Pl}$ is consistent with current bounds. We list relevant experiments and approximate exclusion regions.

Acknowledgments

References

[1] J. R. Eskilt et al., Phys. Rev. D **106**, 063503 (2022), arXiv:2203.01335.

[2] Planck+ACT+SPT+SPIDER joint birefringence (2025), arXiv:2510.25489.

[3] DESI Collaboration, arXiv:2503.14738 (2025).

[4] SPIDER Collaboration, arXiv:2510.25489 (2025).

[5] A. Burinskii, JETP Lett. **118**, 437 (2023).

[6] C. Furey and S. Hughes, Phys. Rev. D **109**, 105001 (2024), arXiv:2409.17948.

[7] S. O. Bilson-Thompson et al., Class. Quant. Grav. **24**, 3975 (2007), arXiv:hep-th/0603022.

[8] C. Furey, Phys. Lett. B **782**, 292 (2018), arXiv:1802.07834.